

On the Azimuthal Alignment of Quasars Spin Vector in Large Quasar Groups and Cosmic Strings.

Reinoud Jan Slagter*

*Asfyon, Astronomisch Fysisch Onderzoek Nederland, 1405EP Bussum
and*

Department of Physics, University of Amsterdam, The Netherlands

(Dated: December 9, 2021)

We find evidence of the alignment of the azimuthal angle of the spin vectors of quasars in their host galaxy in large quasar groups of different redshift. This effect is probably of cosmological origin and could be explained by symmetry breaking of the scalar-gauge field of cosmic strings in the early universe. It is expected that this effect will be more profound for higher redshift.

PACS numbers: 11.27.+d, 11.10.Lm, 11.15.Wx, 12.10.-g, 11.25.-w, 04.50.-h, 04.50.Gh, 04.20.Ha

Keywords: quasar alignment, quasar groups, host galaxy, U(1) scalar-gauge field, cosmic strings

arXiv:2008.09205v3 [gr-qc] 29 Aug 2020

* info@asfyon.com

I. INTRODUCTION

The observation of the structure and objects in our universe at the present epoch, are without doubt related to fundamental processes at the very early stage of that universe, i.e., the Planck scale of $\sim 10^{19} GeV$. It is believed that the universe underwent violent phase-transition during that epoch. One of these processes was the famous Brout-Englert-Higgs (BEH) mechanism. Breaking of the initial symmetry leads to the mass spectrum we observe now. The Higgs particle (or Higgs field), responsible for this breaking, was recently observed at CERN with a mass of $\sim 125 GeV$.

The symmetry breaking can be mathematically elegantly formulated in terms of Lie groups of quantum-chromodynamics ($SU(3)$) and quantum-electro-dynamics ($SU(2) \otimes U(1)$ of the electroweak unification). It is conjectured that even at high enough energy, these groups are sub-groups in a grand unified theory (GUT), first proposed by Georgi and Glashow. It is the hope of many physicists that eventually a quantum-gravity model will emerge, where Einstein's general relativity theory will be unified with quantum mechanics. The features of a black hole, for example, can only be described by a quantum gravity model. The Higgs field Φ is the basis of our Standard Model of particle physics. In fact, this scalar field was already necessary as the order parameter in the theory of superconductivity: the famous and experimentally demonstrated Meissner effect. For a nice overview, see Felsager[1] and Manton[2]. If

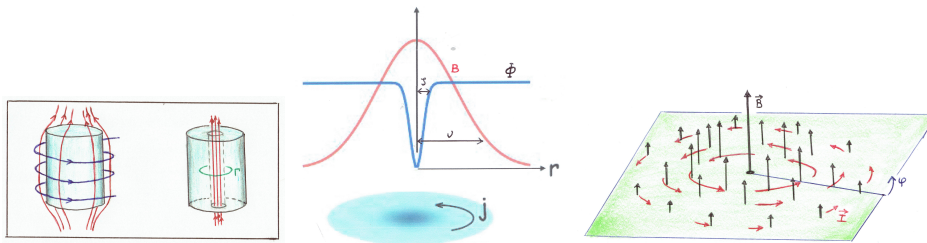


FIG. 1. The formation of quantized vortices. Abrikosov vortex in mixed state of quantized flux lines. Vortex supercurrents are sketched by round arrows in red. The radial dependence of the order parameter Φ is sketched as well as the magnetic field B . In type-II superconductivity the coherence length (ζ) is much smaller than the penetration length (ν).

one places a metal cylinder (or ring) in an external magnetic field and one decreases the temperature below a certain critical temperature, then the magnetic field is expelled from the cylinder. A current is induced in the outer layers of the cylinder, which prevent the magnetic field from penetrating into the outer layers. The magnetic field is described by a gauge potential \mathbf{A} . It is this potential which penetrates into the metal and can change the phases of electrons passing by. When one removes the external magnetic field, then a part of the magnetic field lines is trapped by the surface current. The ring is transformed into a superconducting solenoid. In the superconducting state, there

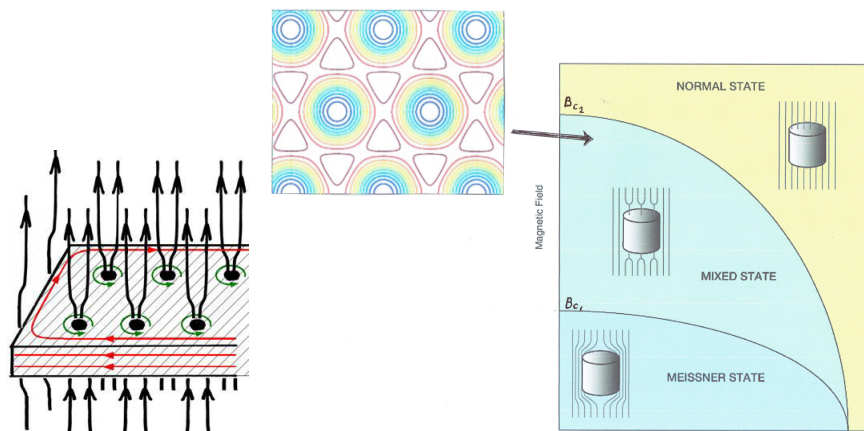


FIG. 2. Left: stable hexagonal Abrikosov lattice in mixed state of quantized fluxes lines. Vortex supercurrents are sketched by round arrows (green). Right: closely packed vortices near the critical region B_{c2}

are Cooper pairs of electrons, which act like bosons, while the electron is a fermion. This "trapping" of magnetic flux happens if the temperature decreases. The superconducting state also depends on the strength of the external magnetic field. If we twist, for example, a solenoid around the superconducting ring and increase the magnetic field,

thin quantized vortices are formed where the normal state of the metal is reestablished. This effect was first observed by Abrikosov[3] and is described by the famous Ginzburg-Landau (GL) equations[4]. See figure 1 and 2.

The same Higgs field enters also in the model of inflationary cosmology, a phase of the universe, where the expansion is described by an exponential function of the cosmological time. This model can explain some obstinate problems in the standard Friedmann-Lemaitre-Robertson-Walker (FLRW) cosmological model, such as the horizon problem. During the GUT phase-transitions a host of exotic objects may have formed, such as monopoles, domain walls and cosmic strings (CS). They are called topological defects and are fully characterized by the scalar-gauge field (Φ, \mathbf{A}) . It were Nielsen and Olesen[5], who first formulated the relativistic string-like object in the abelian Higgs model. They are cylindrical symmetric and topological stable. In this model, which can be extended to Einstein's gravity theory[6, 7], the complex scalar field is written in polar coordinates as $\Phi = \Phi(t, r)e^{in\varphi}$, where the phase contains the azimuthal angle and n is the winding number (topological charge). It determines the phase jump $2\pi n$ when the Higgs field makes a closed curve around the string-like configuration. It is believed that only cosmic strings could survive the rapid expansion of the universe during the inflationary epoch. However, up until today, no experimental evidence of these objects are found and recent measurements of the microwave background power spectrum from COBE and WAMP show that cosmic strings could not provide an adequate explanation for the bulk of density perturbations. Gravitational waves detection will further put stringent bounds on these cosmic strings. Yet it is conjectured that in any field theory which admits cosmic strings, a network of strings inevitable forms at some point during the early universe and persists to the present time[8].

New boost to the field of cosmic strings emerged when it was realized that in string theory (or M-theory) super-massive CS must be formed at an energy scale much higher than the GUT scale. At this scale, the gravitational impact is high, because the CS builds up a huge mass in the bulk spacetime[9, 10]. The warpfactor (or scale factor) will enter the field equations and causes an amplification of the first and second order perturbations of the field variables[11–14].

A possible new phenomenon which could prove the evidence of self-gravitating vortices (or cosmic strings), is the alignment of the spin vector of quasars in their host galaxy in large quasar groups (LQG). The alignment of the position angle of quasars in LQG was observed in the optical range as well as in the radio range and cannot be explained by density perturbations[16, 17]. However, the alignment of the position angle alone is not enough to prove the alignment of the quasar's spin vector. Investigations of the alignment of spin vectors of galaxies in clusters (in the Sloan Digital Sky Survey, SDSS), show some anisotropic distribution[18–20]. However, in large clusters is was found that there is isotropy[21]. This confirms our conjecture that in smaller groups of quasars this alignment will be found and can be explained cosmologically[11–14]. A different explanation was found by Kogai, et al.[22]. The recent observations of already mature galaxies at the early epoch of the universe, i.e., when the cosmos was less than 7 percent of its present age of 13.7 billion years, support the viewpoint that phenomena such as the alignment properties of quasar groups, could be emerge at the early stages of our universe. We shall see in the next sections that the phase parameter φ enters the model of the quasars azimuthal angle alignment in LQG. In section 2 we summarize the theoretical model and in section 3 we depict for four LQG the azimuthal angle of the spin vector.

II. SUMMARY OF THE MODEL

When gravity comes into play at very small scales and during the phase transition, one can write the FLRW spacetime as

$$ds^2 = \mathcal{W}(t, r, y)^2 \left[e^{2(\gamma(t, r) - \psi(t, r))} (-dt^2 + dr^2) + e^{2\psi(t, r)} dz^2 + r^2 e^{-2\psi(t, r)} d\varphi^2 \right] + dy^2, \quad (1)$$

where y represents the extra dimension, $\mathcal{W}(t, r, y)$ the warpfactor or dilaton field[11].

The complex scalar (Higgs) field and gauge field A_μ (Maxwell field) are written as

$$\Phi = \Phi(t, r)e^{in\varphi}, \quad A_\mu = \frac{n}{e} [P(t, r) - 1] \nabla_\mu \varphi. \quad (2)$$

where n also determines the magnetic flux of the vortex, which is quantized by $\frac{2\pi n}{e}$.

If one writes out the field equations, then the azimuthal angle φ will of course not enter the PDE's, because the model is axially symmetric. If the axially symmetry is dynamically broken, an off-diagonal metric function will appear, i.e., $g_{t\varphi}$. The spacetime will then possess 2 instead of 3 Killing vectors. It are quantum fluctuations which excites the vortex.

It is remarkable that this symmetry breaking is comparable with the phase transition in type II superconductivity, considered in our model. Self-gravitating objects in GRT in equilibrium exhibit also analogue with the mathematical model of the MacLaurin-Jacobi sequences and its bifurcation points[23].

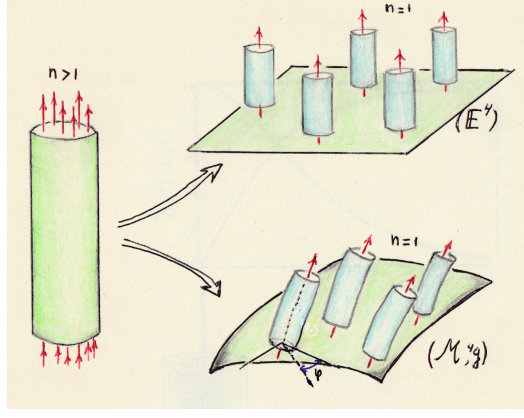


FIG. 3. *Excitation and decay of a high multiplicity vortex into correlated vortices of unit flux $n = 1$. Top: the Abrikosov lattice in Euclidean space. Bottom: correlated vortices with preferred azimuthal angle φ in curved spacetime after the symmetry breaking.*

After the excitation, the vortex configuration returns to its original axially symmetric situation, but an imprint will be left over in the azimuthal dependency of the orientations of the clustering of Abrikosov vortices lattice. It is caused by the fact that the energy of the vortex is proportional with n^2 . So there can be no exact ground state for the string carrying multiple flux quanta. For $n=1$ we have the minimal energy situation, which is stable as it cannot decay into topological trivial field. See figure 3. The topological charge can also be seen as the net number of new type of particles.

The excitation can be best described in an approximation scheme, were we expand the field variables as

$$\begin{aligned} g_{\mu\nu} &= \bar{g}_{\mu\nu}(\mathbf{x}) + \frac{1}{\omega} h_{\mu\nu}(\mathbf{x}, \xi) + \frac{1}{\omega^2} k_{\mu\nu}(\mathbf{x}, \xi) + \dots, \\ A_\mu &= \bar{A}_\mu(\mathbf{x}) + \frac{1}{\omega} B_\mu(\mathbf{x}, \xi) + \frac{1}{\omega^2} C_\mu(\mathbf{x}, \xi) + \dots, \\ \Phi &= \bar{\Phi}(\mathbf{x}) + \frac{1}{\omega} \Psi(\mathbf{x}, \xi) + \frac{1}{\omega^2} \Xi(\mathbf{x}, \xi) + \dots, \end{aligned} \quad (3)$$

where we write the subsequent orders of the scalar field as[15]

$$\bar{\Phi} = \eta \bar{X}(t, r) e^{in_1 \varphi}, \quad \Psi = Y(t, r, \xi) e^{in_2 \varphi}, \quad \Xi = Z(t, r, \xi) e^{in_3 \varphi}. \quad (4)$$

$1/\omega$ represents the expansion parameter in the so-called multiple-scale approximation[24–26].

The relevant energy-momentum tensor components are

$${}^4T_{t\varphi}^{(0)} = \bar{X} \bar{P} \dot{Y} n_1 \sin[(n_2 - n_1)\varphi], \quad (5)$$

$${}^4T_{\varphi\varphi}^{(0)} = e^{-2\gamma} r^2 \dot{Y} (\partial_t \bar{X} - \partial_r \bar{X}) \cos[(n_2 - n_1)\varphi] + \frac{n_1 e^{2\bar{\psi} - 2\bar{\gamma}}}{\bar{W}_1^2 e} \dot{B} (\partial_r \bar{P} - \partial_t \bar{P}), \quad (6)$$

$${}^4T_{tt}^{(0)} = \dot{Y}^2 + \dot{Y} (\partial_t \bar{X} + \partial_r \bar{X}) \cos[(n_2 - n_1)\varphi] + \frac{e^{2\bar{\psi}}}{\bar{W}_1^2 r^2 e} \left(e \dot{B}^2 + n_1 \dot{B} (\partial_r \bar{P} + \partial_t \bar{P}) \right), \quad (7)$$

while the background term ${}^4\bar{T}_{t\varphi} = 0$. We conclude that the axially symmetry is broken already to first order: the azimuthal angle (φ) dependency appears in the first and second order terms. In the expression for ${}^4T_{tt}^{(0)}$ we observe that the scale factor \bar{W}_1 enters the denominator. So if the scale increases, the contribution of the $\cos[(n_2 - n_1)\varphi]$ will become dominant. In the second order terms there appear terms like $\cos(n_3 - n_2)\varphi$ [13]. These terms have extrema which differ $\text{mod}(\frac{\pi}{n})$. After the excitation of the vortex with multiplicity n , it will decay into n vortices of unit flux in a regular lattice (just as the Abrikosov vortices form a hexagonal lattice such that the energy is minimal). The calculation of the forces between the vortices is complicated by the gravitational contribution. In the Bogomol'nyi[27] approximation, where the masses of the Higgs and gauge particles are equal, one proves that there is equilibrium. In general, one must solve the time dependent GL equations, which can only be done numerically. From the expression of ${}^4T_{t\varphi}^{(0)}$, we conclude that when the configuration returns to its original ground state and $n_2 = n_1 = 1$

($\sin(n_2 - n_1)\varphi \rightarrow 0$) and the axially symmetry is restored to first order. The term $\cos(n_2 - n_1\varphi)$ in ${}^4T_{\varphi\varphi}^{(0)}$ has its maximum. So there is an emergent imprint of a preferred azimuthal angle φ on the lattice of vortices when the ground state is reached ($n=1$).

III. THE QUASAR CONNECTION

We gathered quasar data from the NASA/IPAC extragalactic database (NED) and SIMBAD database. We investigated 4 LQG (see Park, et al.[28]) with a average redshift of $z = 1.55, 1.51, 1.06$ and 0.74 . We extract the position angle (p) and eccentricity (ϵ) of the host galaxy. The data are based on the assumption that $H_o = 73.0, \Omega_M = 0.27$ and $\Omega_{vac} = 0.73$. In order to obtain the 3-dimensional orientation of the spin vector (SV), one calculates the inclination

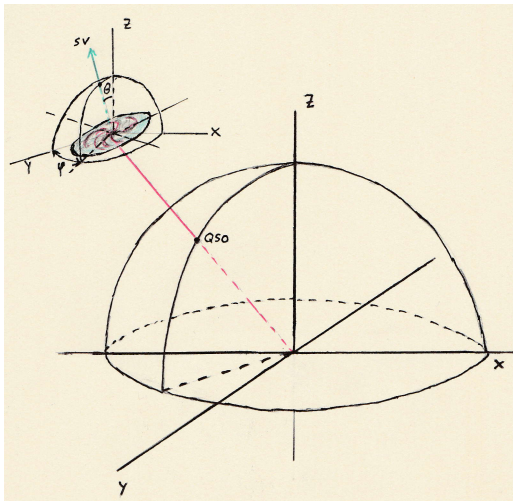


FIG. 4. Visualization of the spin vector of a quasar as determined by the azimuthal angle φ and polar angle θ .

(i), the azimuthal angle (φ) and polar angle (θ) by the relations (1986, Flin, et al.)

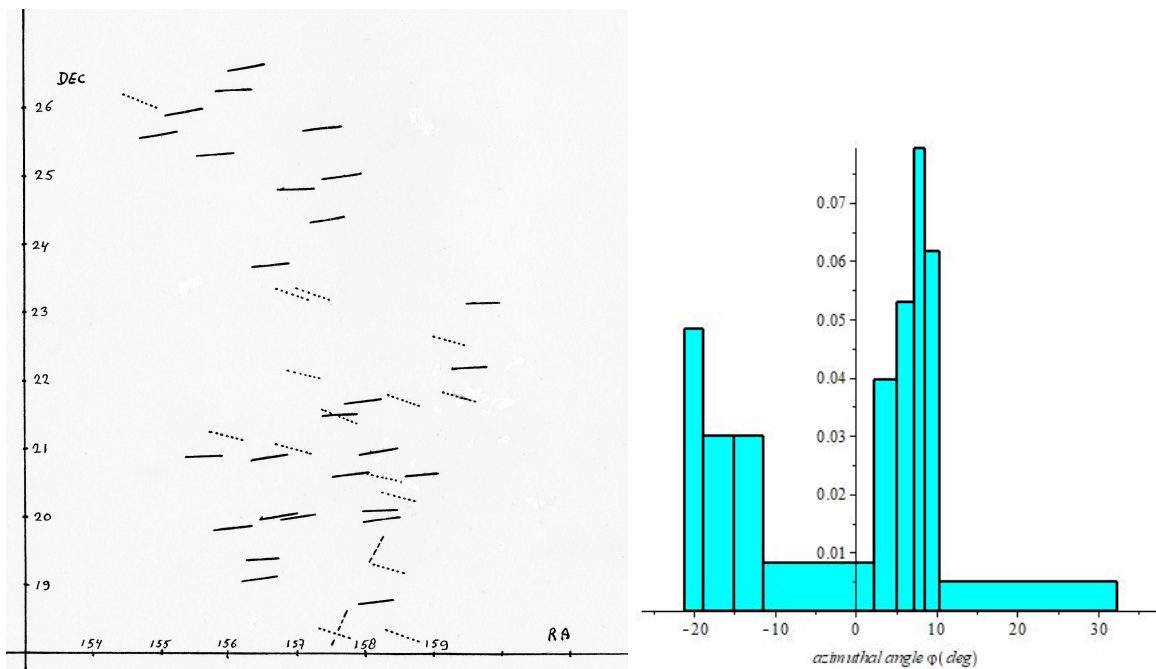


FIG. 5. Distribution of the azimuthal angle in LQG-18 with average redshift 1.49. $N = 45$.

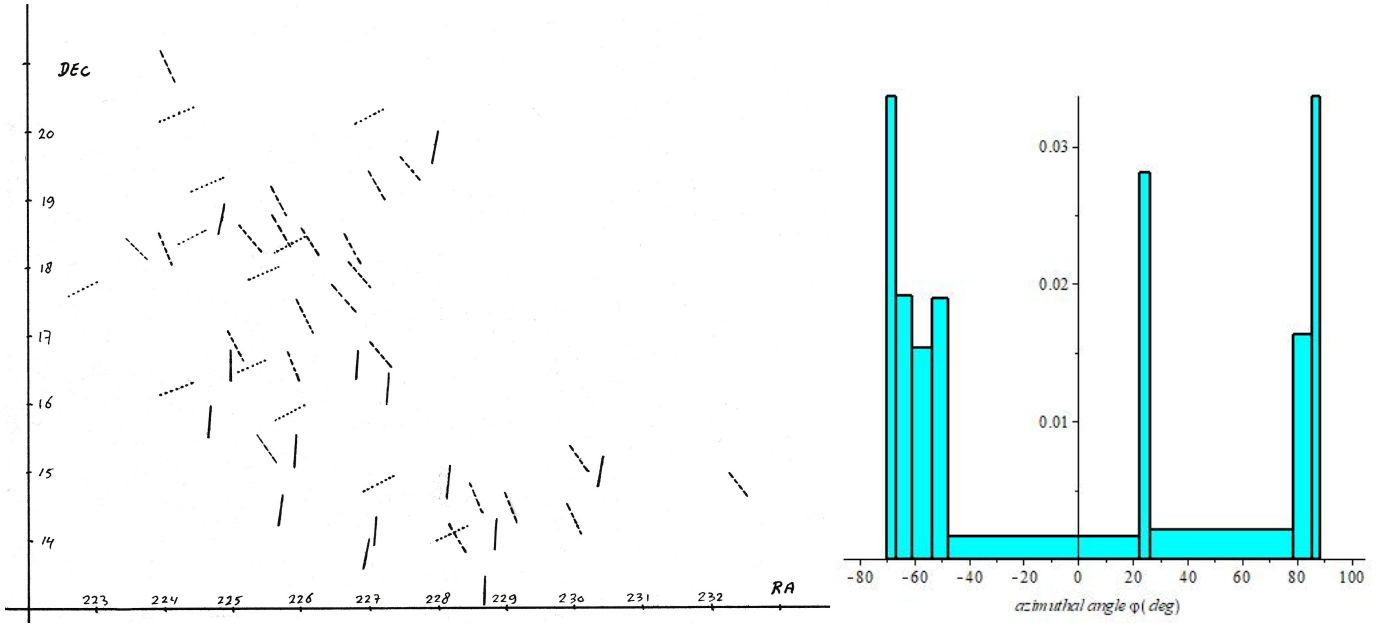


FIG. 6. Distribution of the azimuthal angle in LQG-12 with average redshift 1.06. $N = 51$.

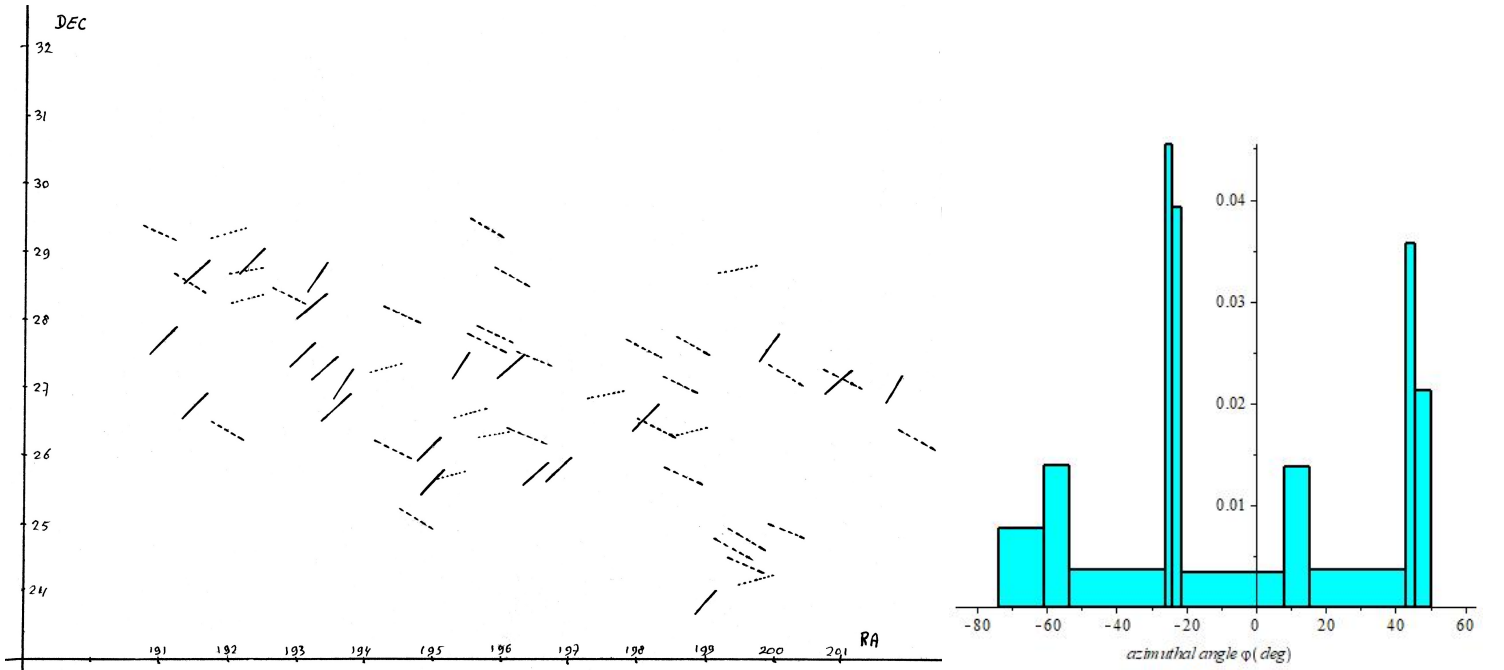


FIG. 7. Distribution of the azimuthal angle in LQG-4 with average redshift 1.55. $N = 62$.

$$\cos^2 i = \frac{\epsilon^2 - \epsilon_0^2}{1 - \epsilon_0^2} \quad (8)$$

$$\sin \theta = -\cos i \sin \delta \pm \sin i \sin p \cos \delta \quad (9)$$

$$\sin \varphi = \frac{-\cos i \cos \delta \sin \alpha + \sin i (\mp \sin p \sin \delta \sin \alpha \mp \cos p \cos \alpha)}{\cos \theta} \quad (10)$$

There are four solutions for every quasar SV, (φ_1, θ_1) , (φ_2, θ_2) , $(-\varphi_1, \theta_3)$, $(-\varphi_2, \theta_4)$, where $|\theta_1 + \theta_2| = \pi$ and $|\theta_3 + \theta_4| = \pi$. We will made a choice between the two orientations of the azimuthal angle φ , using the conjecture that there will be

two peaks with different height (see theory of section 2). So we don't count for all the possible orientations, as is done by other authors (for example, Aryal, et al., 2008).

In the figures 5-8 we plotted the orientations and the histograms for the 4 different redshifts.

Without statistical analysis, it is evident that in all the four LQG there are preferable azimuthal directions with different peaks.

It is conjectured by the theoretical explanation of section 2, that the peaks in the azimuthal angle distribution are out of phase, and are determined by trigonometrical functions $\sin(n_i - n_j)\varphi$ and $\cos(n_i - n_j)\varphi$ in the successive terms of ${}^4T_{t\varphi}$ and ${}^4T_{\varphi\varphi}$. n_i are the multiplicities of subsequent perturbation terms of the scalar field. In figure 7 we see a nice example of the two different peaks.

The next task is to determine the peak heights and to compare these peaks with the theoretical prediction. More accurate data will then be necessary for high redshift.

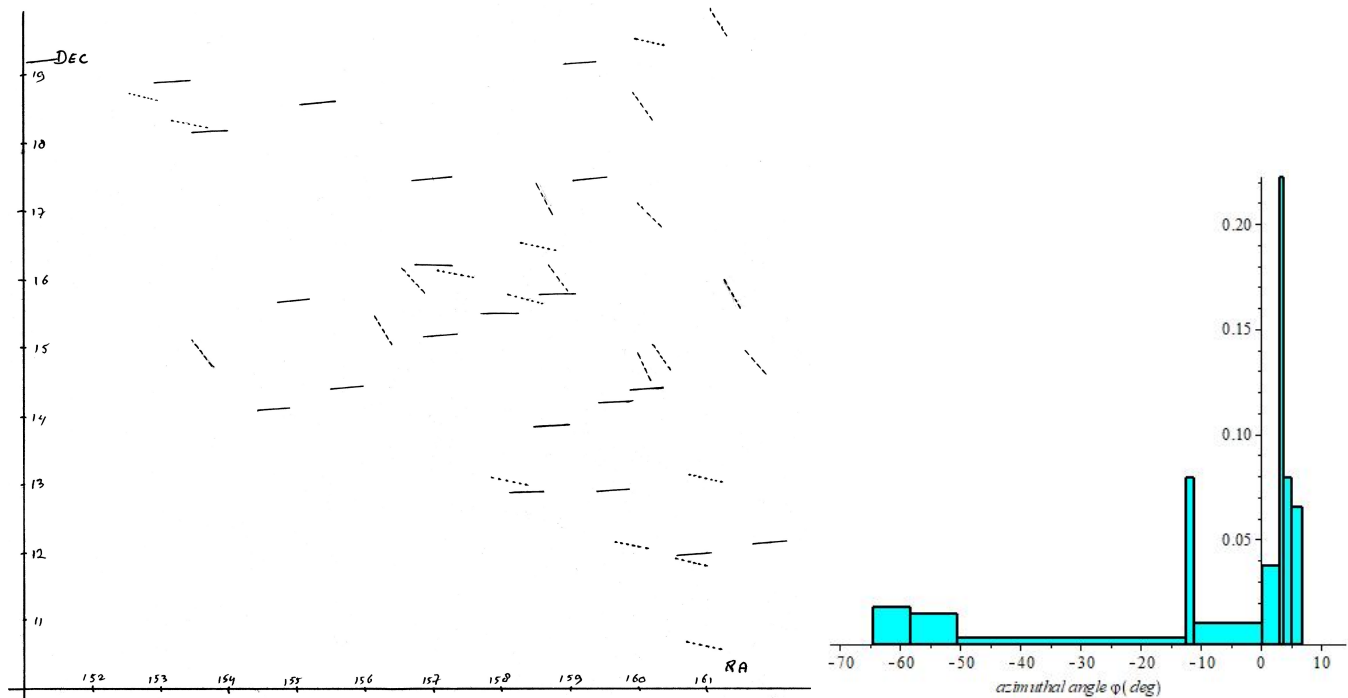


FIG. 8. Distribution of the azimuthal angle in LQG-19 with average redshift 0.74. $N = 45$.

IV. CONCLUSIONS

It is found that the azimuthal angle of the spin vector of quasars in their host galaxies in the four quasar groups under consideration, show preferred directions. This can be explained by an emergent azimuthal angle dependency of the Nielsen-Olesen vortices just after the symmetry breaking at GUT scale. A throughout investigation of more LQG at higher redshift will be necessary, in order to confirm the trigonometrical distribution of the azimuthal angle of the several orders in the approximation.

V. APPENDIX: THE DATA GENERATION

The calculation of the two angles θ, φ from the host galaxies of the five quasar groups, i.e., right ascension (δ), declination (α), eccentricity ($\epsilon = a/b$; a, b the major and minor axes of the ellipse), and position angle (p), can be done with a short Maple program. The quasar data for LQG19, for example, are written in the file LQG19. It is a $(N,5)$ matrix, with N the number of quasars in the group. Note that we work in Maple in radians.

```

restart;
H := Array(readdata("C:/LQG19.txt", 1, 2, 3, 4, 5));
M := Array(1 .. 45);
for i to 45 do M[i] := H(i, 4)/H(i, 3) od;
K := Array(1 .. 45);
L1 := Array(1 .. 45); L2 := Array(1 .. 45);
for i to 45 do K[i] := cos(e) = sqrt((M[i]^2 - 0.04))/.96; L1[i] := solve(K[i], e) od;
for i to 45 do K[i] := cos(e) = -sqrt((M[i]^2 - 0.04))/.96; L2[i] := solve(K[i], e) od;
R1 := Array(1 .. 45); R2 := Array(1 .. 45);
S1 := Array(1 .. 45); S2 := Array(1 .. 45);
for i to 45 do R1[i] := {sin(phi) = (-cos(L1[i])*cos(H[i, 2]*(pi/180))*sin(H[i, 1]*(pi/180))
+sin(L1[i]*(-sin(H[i, 5]*(pi/180))*sin(H[i, 2]*(pi/180))*sin(H[i, 1]*(pi/180))
-cos(H[i, 5]*(pi/180))*cos(H[i, 1]*(pi/180))))/cos(theta), sin(theta) =
-cos(L1[i])*sin(H[i, 2]*(pi/180))+sin(L1[i])*sin(H[i, 5]*(pi/180))*cos(H[i, 2]*(pi/180))};
R2[i] := solve(R1[i], {phi, theta} od
for i to 45 do S1[i] := {sin(phi) = (-cos(L2[i])*cos(H[i, 2]*(pi/180))*sin(H[i, 1]*(pi/180))
+sin(L2[i]*(-sin(H[i, 5]*(pi/180))*sin(H[i, 2]*(pi/180))*sin(H[i, 1]*(pi/180))
-cos(H[i, 5]*(pi/180))*cos(H[i, 1]*(pi/180))))/cos(theta), sin(theta) =
-cos(L2[i])*sin(H[i, 2]*(pi/180))+sin(L2[i])*sin(H[i, 5]*(pi/180))*cos(H[i, 2]*(pi/180))};
S2[i] := solve(R1[i], {phi, theta} od

```

As a result, one can fill the tabel:

TABLE I. Data for LQG-19.

Ra	Dec	z	a	b	p	ϵ	i	(φ, θ)
152.66153	18.72273	.745	5.25	4.88	123	.93	.386, 2.76	(39.3, 0.11) (12.6, 36.7)
153.21761	18.94306	.766	6.71	5.84	179	.87	.527, 2.62	(58.4, -164.3) (4.8, 163.2)
151.12213	19.23613	.757	5.76	5.13	129	.89	.483, 2.66	(45.9, 2.81) (6.8, 39.3)
...

-
- [1] Felsager, B. (1987) *Geometry, particles and fields*. Odense University press: Odense, Denmark.
 - [2] Manton, N. and Sutcliffe, P. (2007) *Topological solitons*. Cambridge University press, Cambridge, UK.
 - [3] Abrikosov, A. A. (1957) *Soviet Physics JETP* **5**, 1774, 1957.
 - [4] Ginzburg, V. L. and Landau, L. D. (1950) *Zh. Eksp. Teor. Fiz.* **20**, 1064.
 - [5] Nielsen, H.B. and Olesen, P. (1973) *Nucl. Phys.* **B61**, 45.
 - [6] Anderson, M.R. (2003) *The Mathematical Theory of Cosmic Strings*. IoP publishing, Bistol, UK.
 - [7] Garfinkle, D. (1985) *Phys. Rev.* **D32**, 1323.
 - [8] Vilenkin, A. and Shellard, E.P.S. (1994) *Cosmic Strings and Other Topological Defects*. Cambridge University press, Cambridge, UK.
 - [9] Randall, L. and Sundrum, R. (1999) *Phys. Rev. Lett.*, **83**, 3370.
 - [10] Randall, L. and Sundrum, R. (1999) *Phys. Rev. Lett.* **83**, 4690.
 - [11] Slagter, R.J. and Pan, S. (2016) *Found. of Phys.* **46**, 1075.
 - [12] Slagter, R.J. (2016) *J. of Mod.Phys.* **7**, 501.
 - [13] Slagter, R.J. (2017) *J. of Mod.Phys.* **8**, 163.
 - [14] Slagter, R.J. (2018) *Int. J. of Mod.Phys.D* **27**, 1850094.
 - [15] Slagter, R. J. (2017) *Spacetime Physics 1907-2017*. Minkowski Inst. Press, Montreal, Canada.
 - [16] Hutsemekers, D., Braibant, L., Pelgrims, V. and Sluse, D. (2014) *Astron. Astrophys.* **572**, A18.
 - [17] Taylor, A.R. and Jagannathan, P. (2016) *Mon. Not. Roy. Astr. Soc.* **459**, 459, L36.
 - [18] Flin, P. and Godlowski, W. (1986) *Mon. Not. R. astr. Soc.* **222**, 525.
 - [19] Aryal, B., Kafle, P. R. and Saurer, W. (2008) *Mon. Not. R. astr. Soc.* **389**, 741.
 - [20] Yadav, S. N., Aryal, B. and Saurer, W. (2016) arXiv: astro-ph/160602881.
 - [21] Yadav, S. N., Aryal, B. and Saurer, W. (2017) *Res. in Astron. Astrophys.* **17**, 64.
 - [22] Kogai, K., Matsubara, T., Nishizawa, A. J. and Urakawa, Y. (2018) *J. Cosm. Astropar. Phys.* **14**, 101088. Canada.
 - [23] Lebovitz, N. R. (1967) *Bifurcation and stability problems in astrophysicsm*, in *Applications of bifurcation theory*. Academic Press, New York, USA
 - [24] Choquet-Bruhat, Y. (1969) *Commun. Math. Phys.* **12**, 16.

- [25] Choquet-Bruhat, Y. (1977) *Gen. Rel. Grav.* **8**, 561.
- [26] Slagter, R. J. (2001) *Class. and Quantum Grav.* **18**, 463
- [27] Bogomol'nyi, E. (1976) *Sov. J. Nucl. Phys.* **24**, 449.
- [28] Park, C., Song, H., Einasto, M., Lietzen, H. and Heinamaki, P. (2015) *J. Korean Astr. Soc.* **48**,75.